

Proceedings of the Second Annual LHCP

October 16, 2018

Experimental Summary

ALEANDRO NISATI

*Istituto Nazionale di Fisica Nucleare
P.le A. Moro 2, Rome, 00185, Italy*

ABSTRACT

High-quality results have been produced with the first Large Hadron Collider run on high- p_T , heavy flavour and heavy ion physics. These results, as well as the most recent data analyses from Tevatron, have been presented and discussed at the LHCP2014 conference. A selection of some of them is summarised in this paper, with care to those that stimulated interesting discussions during this event.

PRESENTED AT

The Second Annual Conference
on Large Hadron Collider Physics
Columbia University, New York, U.S.A
June 2-7, 2014

1 Introduction

During the conference so many interesting talks and nice results have been presented, that would be impossible to properly summarize them in a single paper. Therefore, a selection is here summarised, with particular attention to those that stimulated interesting discussions during this workshop.

2 Electroweak and QCD physics

A very wide set of studies on Standard Model (SM) have been presented and discussed in this conference. These range from QCD jet measurements to measurements of photons, leptons, single vector boson and vector boson pair production at the Large Hadron Collider (LHC) and Tevatron. For single inclusive object studies, the overall uncertainty on measured quantities is dominated by the experimental and theory systematics. On the contrary, boson pair measurements are almost equally limited by statistical and systematic uncertainties. In all cases, Monte Carlo predictions show a good agreement with next-to-leading order (NLO) or next-to-next-to-leading order (NNLO) calculations.

Vector boson pair production is an important physics process as it represents one of the most relevant background source to new physics searches. Furthermore, it allows the study of the gauge boson couplings, probing the realization in nature of anomalous couplings as predicted by theories beyond SM. Quartic anomalous couplings (AQGC) have been searched for at Tevatron and LHC, studying for example the production of $WW\gamma$ and $WZ\gamma$ events, as reported in reference [1].

The Vector Boson Scattering (VBS) is a key process to probe the nature of the electroweak symmetry breaking mechanism. It is of paramount importance to understand whether the SM-like Higgs boson recently discovered at LHC [20][21] is the only process responsible of the unitarization of this process, or whether, as predicted by many beyond-Standard-Model scenarios (BSM), other physics reactions contribute to the VV ($V=W,Z$) scattering amplitude. A first measurement of same charge $W^\pm W^\pm jj$ vector boson production processes has been made by ATLAS using 20.3 fb^{-1} of data at $\sqrt{s} = 8 \text{ TeV}$ [2]. In the data analysis, two signal regions have been defined, one loose (inclusive) dedicated to measure the QCD production, and the second to extract the electroweak contribution; see figure 1 (left). An excess of events has been found in both regions, providing 4.5 and 3.6 standard deviations (s.d.) evidence for QCD and electroweak production, respectively.

The knowledge of parton distribution functions (PDFs) represents an important limitation to the measurement of 125 GeV Higgs boson physics properties, in particular for the couplings to elementary particles. In fact, they contribute together with the uncertainties associated to the factorization and renormalization scale, to an uncertainty that is already comparable to the experimental uncertainty (see also section 5). With increasing integrated luminosity at the LHC, the overall systematic uncertainty will be quickly dominated by theory errors. This represents an important motivation for the improvement of the accuracy of PDF measurements in the near future. Though recently proposed electron-hadron experiments would be in best position to extract PDF information, Tevatron and LHC data can provide important constraints to PDFs. Studies in this direction already started, and an example is available in reference [3]: figure 1 (right) shows the reduction obtained in an analysis of gluon PDFs where the measured production cross sections at Tevatron and LHC are used.

3 Top quark physics

The production cross section of $t\bar{t}$ pairs and single top quark has been measured at $\sqrt{s}= 1.96 \text{ TeV}$ in $p\bar{p}$ and pp collisions up to 8 TeV in the centre-of-mass energy. The global uncertainty is about 8% (5%) at $\sqrt{s}=7 \text{ TeV}$ (8 TeV), per experiment (ATLAS, CMS), and 5% at $\sqrt{s}= 1.96 \text{ TeV}$ (CDF, D0). The data are in agreement with theory predictions within experimental and theoretical accuracy. A nice $t\bar{t}$ production cross-section summary is shown in figure 2 (left).

One of the most important set of results shown at the conference concerns the recent studies of single top production at hadron colliders. There are three main processes for the production of this quark in single-mode: s-channel, t-channel and Wt channel. In the s-channel, a quark anti-quark annihilate to produce a

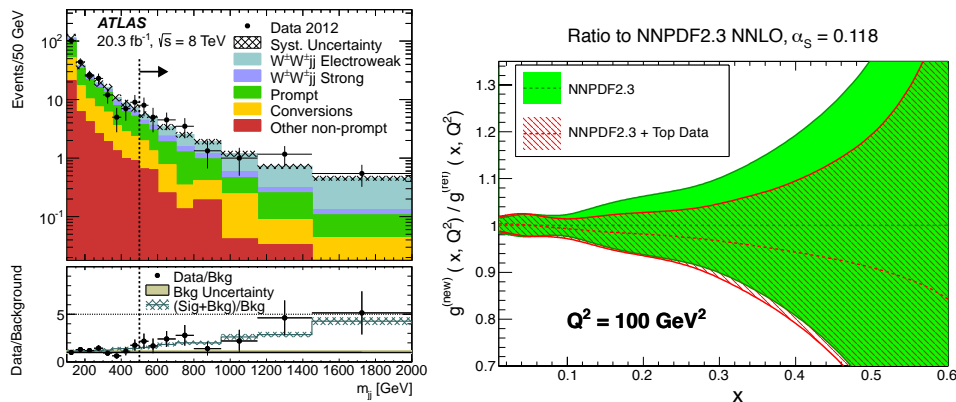


Figure 1: Left: The jet-jet invariant mass m_{jj} distribution for events passing the inclusive region selections except for the m_{jj} selection indicated by the dashed line. The $W^\pm W^\pm jj$ events on the left of the dashed line are mainly from strong production, while those on the right are produced mainly by electroweak processes. The black hatched band in the upper plot represents the systematic uncertainty on the total prediction. On the lower plot the shaded band represents the fractional uncertainty of the total background while the solid line and hatched band represents the ratio of the total prediction to background only and its uncertainty. The $W^\pm W^\pm jj$ prediction is normalized to the SM expectation. Right: The ratio of the NNPDF2.3 NNLO gluon PDF at $Q^2 = 100 \text{ GeV}^2$ between the default fit and after including the Tevatron and LHC top quark cross section data [3].

top-anti-beauty quark pair; in the t-channel, an initial state quark interacts with a gluon, emitting a top-anti-beauty quark pair in association with a quark in the final state; finally, in the Wt channel a b-quark from the sea interacts with a initial state gluon producing a top quark in association with a W boson. It should be noted that the Wt production is not accessible at Tevatron because of the small production cross section in proton-anti-proton collisions at $\sqrt{s} = 1.96 \text{ TeV}$. The experiment D0 first observed the t-channel process at Tevatron. At the LHC, the t-channel has been measured by ATLAS and CMS with an overall accuracy smaller than 15% [4][5]. The Wt process has been observed with a significance of 6.1 s.d. by CMS [6] and with 4.2 s.d. by ATLAS [7]. No significant deviation from Standard Model predictions has been observed in any of the two processes above summarized. The single top production in the s-channel has been observed at Tevatron: the combination of the results from CDF and D0 has produced the first observation of this process with a significance of 6.3 s.d.; also in this case, data are in good agreement with Standard Model predictions within theoretical and experimental uncertainties [10]. On the contrary, this process has not been observed yet at the LHC, and upper limits on its production cross-section have been set [8][9].

The measured top mass world combination is $m_t = 173 \pm 0.76 \text{ GeV}$ [11]. The combination has been performed using the BLUE package, and efforts are ongoing to harmonize the treatment of the systematic uncertainties. CDF and D0 reported the final top mass measurements, $m_t = 173.16 \pm 0.57(\text{stat}) \pm 0.74(\text{syst}) \text{ GeV}$ and $m_t = 174.98 \pm 0.58(\text{stat}) \pm 0.49(\text{syst}) \text{ GeV}$ respectively, while CMS has updated previous measurements ($m_t = 172.22 \pm 0.14(\text{stat}) \pm 0.72(\text{syst}) \text{ GeV}$).

One of the most discussed topics during this conference on top physics was certainly the understanding of the relation between the top mass measured experimentally in hadron collisions to the pole mass, which enters the Standard Model prediction of processes involving top quarks. A nice overview of the problem has been given, and a discussion on how to evaluate the uncertainty on the connection between the measured quantity and the pole mass used in the theory [12] has been made. In summary, the top quark mass uncertainty in hadron colliders $\Delta m_t(th)$ is given by the combination of a term $\Delta m_t(MC \rightarrow MSR)$ due to the conversion from the MC mass to the “short-range” mass (MSR), and a offset $\Delta m_t(MSR \rightarrow pole)$ that converts the short-range mass to the pole mass [13]. In the report given at the conference, $\Delta m_t(MC \rightarrow MSR) \sim \pm 0.7 \text{ GeV}$ and $\Delta m_t(MSR \rightarrow pole) \sim +0.5 \text{ GeV}$.

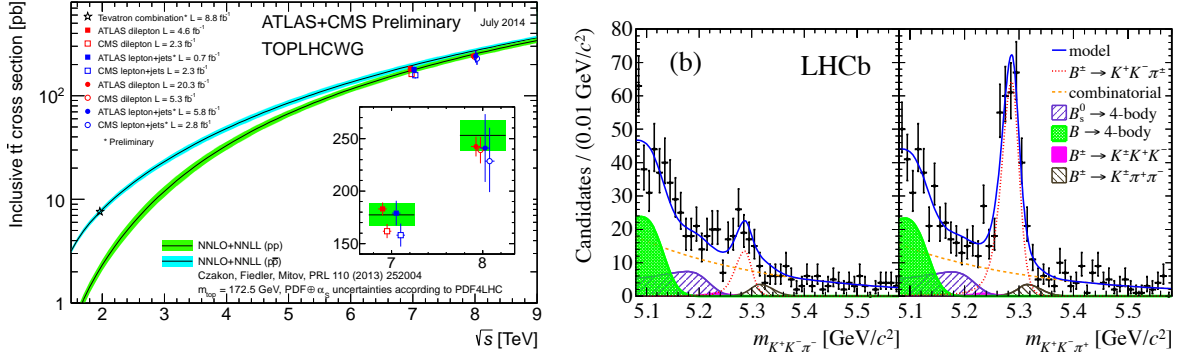


Figure 2: Left: Summary of LHC and Tevatron measurements of the top-pair production cross-section as a function of the centre-of-mass energy compared to the NNLO QCD calculation complemented with the next-to-next-to-leading log (NNLL) resummation (top++2.0). The theory band represents uncertainties due to renormalisation and factorisation scale, parton density functions and the strong coupling. The measurements and the theory calculation is quoted at the top mass $m_t=172.5$ GeV (measurements made at the same centre-of-mass energy are slightly offset for clarity). Right: Invariant mass spectra of $B^\pm \rightarrow K^+K^-\pi^\pm$ decays in the region $m_{K^+K^-}^2 < 1.5$ GeV². The left-hand panel shows the B^- modes and the right-hand panel shows the B^+ modes. The results of the unbinned maximum likelihood fits are overlaid [16].

4 Heavy flavour physics

The non-invariance of the combined asymmetry of charge conjugation and parity, known as CP violation, is described in the Standard Model by the Cabibbo-Kobayashi-Maskawa quark-mixing matrix [14][15]. Charmless decays of B mesons to three hadrons offer the possibility to investigate CP asymmetries that are localized in phase space, as these decays are dominated by intermediate two-body resonant states. Moreover, the $B^\pm \rightarrow K^+K^-\pi^\pm$ decay is interesting because $s\bar{s}$ contributions are strongly suppressed. The LHCb experiment has reported measurements of the inclusive CP-violating asymmetries for $B^\pm \rightarrow \pi^+\pi^-\pi^\pm$ and $B^\pm \rightarrow K^+K^-\pi^\pm$ decays. For the first time, an evidence for this asymmetry with a significance of 3.2 s.d. has been found [16]. Figure 2 (right) shows the rate asymmetry of $B^\pm \rightarrow K^+K^-\pi^\pm$ decays.

This evidence, along with the recent evidence for CP violation in the $B^\pm \rightarrow K^\pm\pi^+\pi^-$ and $B^\pm \rightarrow K^\pm K^+K^-$ decays [17] and recent theoretical developments, indicates new mechanisms for CP asymmetries, which should be included in models for future amplitude analyses of charmless three-body decays.

Violations of CP symmetry are predicted to be small in charm decays, but could be enhanced in the presence of non-SM physics. Direct CP violation arises when two or more amplitudes with different weak and strong phases contribute to the same final state. This is possible in singly Cabibbo-suppressed $D^0 \rightarrow K^-K^+$ and $D^0 \rightarrow \pi^-\pi^+$ decays where significant penguin contributions can be expected [18]. To date, CP violation in charm decays has not been established experimentally. CP asymmetries have been recently investigated by the LHCb collaboration measuring the asymmetry ΔA_{CP} , for the two decays above. No observation of CP violation has been shown at the level of $\Delta A_{CP} \sim 10^{-3}$ [19]. This represents the most precise measurement of time-integrated CP asymmetries in the charm sector from a single experiment.

Lots of studies have been discussed on heavy-flavour spectroscopy. The observation of the particle $Z(4430)$ by LHCb has been shown with a significance in excess of 14 s.d.; this object was already observed by the experiment Belle in 2008, but with no conclusion from the experiment BaBar. Also, evidence for the decay $X(3872) \rightarrow \psi(2S)\gamma$ has been presented. B_c physics studies have produced many results, in particular, LHCb has performed the most precise measurement of the B_c^\pm hadron lifetime, using the decay channel $B^\pm \rightarrow J/\psi \mu^\pm \nu$: $\tau = (509 \pm 8(stat) \pm 12(syst))$ fs.

channel	ATLAS-old	ATLAS-Run1	CMS
$H \rightarrow \gamma\gamma$	$126.8 \pm 0.2 \pm 0.7$	$125.98 \pm 0.42 \pm 0.28$	$125.4 \pm 0.5 \pm 0.6$
$H \rightarrow ZZ^{(*)} \rightarrow llll$	$124.3^{+0.6}_{-0.5} \text{ }^{+0.5}_{-0.3}$	$124.51 \pm 0.52 \pm 0.04$	$125.6 \pm 0.4 \pm 0.2$
Combination	$125.5 \pm 0.2 \text{ }^{+0.5}_{-0.6}$	$125.36 \pm 0.37 \pm 0.18$	$125.7 \pm 0.3 \pm 0.3^{(*)}$

Table 1: Higgs boson mass measurements, in GeV, from ATLAS and CMS at the time of this conference. As long as ATLAS is concerned, final results from Run1 analysis are reported, compared to those previously available. For each measurement the first error represents the statistical uncertainty, while the second is the overall systematic uncertainty. (*) The CMS combined mass has not been updated with the new measurement from the $H \rightarrow ZZ^{(*)} \rightarrow llll$ channel, and the value available in reference [26] has been reported.

5 The 125 GeV Higgs boson and BSM Higgs boson searches

One of the most discussed subjects during this conference was the final “125 GeV” Higgs boson [20][21] mass measurement by ATLAS, based on the data collected in the first run of LHC. The measurement is based on the analysis of inclusive channels $H \rightarrow \gamma\gamma$ and $H \rightarrow ZZ^{(*)} \rightarrow llll$ and it has been performed after the new electron and photon energy calibration using the data from the first LHC run [23]. This new calibration relies on improved corrections of the calorimeter non-uniformities and layer inter-calibration based on electron/photon/muon data, individual electromagnetic cluster energy correction using multi-variate methods, and an improved calorimeter energy-scale and energy-resolution determination using high statistics of $Z \rightarrow ee$ decays.

The results, together with a new categorization of the $H \rightarrow \gamma\gamma$ final states, based on the full 2011 and 2012 data sets, are summarized in Table 1[22], together with the most up to date results from CMS [24][25][26]. At the time of the writing of these proceedings, CMS has reported a new Higgs boson mass measurement where the latest results on $H \rightarrow \gamma\gamma$ and $H \rightarrow ZZ^{(*)} \rightarrow llll$ are used in the combination [27]. The consistency between the ATLAS mass measurements in the diphoton channel and in the 4-lepton channel is about 2 standard deviations. Furthermore, the systematic uncertainty in the ATLAS combined measurement has decreased by a factor 3 thanks to the more accurate electron and photon calibration.

Impressive results have been produced also from the study of the Higgs boson couplings to elementary particles. This includes also the search for this scalar in two-fermion final states, in particular $H \rightarrow b\bar{b}$ and $H \rightarrow \tau\tau$ decays. Evidence of the production and decay of this particle in these final states has been shown by ATLAS and CMS with a significance of 3.7 s.d. [29] and 4.4 s.d. [28], respectively. The signal strength μ , which is the ratio between the measured Higgs production and decay rate to the one expected from the Standard Model, has been measured by ATLAS to be $\mu = 1.30 \pm 0.12(\text{stat})^{+0.14}_{-0.11}(\text{syst})$; theory uncertainty (mainly from parton distribution functions, PDFs, and QCD factorization and renormalization scale) are comparable to those from experimental sources. Similar results have been shown by CMS. The signal rate from different production mechanisms and different decay channels have been used to extract the Higgs boson couplings to elementary fermions and bosons. Several coupling models have been studied, following the prescription and the recommendations published in [30]. The results have been obtained assuming that only Standard Model particles contribute to the total natural width, and to the production and decay loops. These findings have shown good agreement with Standard Model predictions. An example of a particular model is shown in figure 3 (left), where 6 coupling parameters are studied simultaneously. In this particular model it is possible to see that couplings are measured with an accuracy of the order 20% - 50%. The analysis of events with a Z-boson produced in association with large missing transverse energy can be used to search for ZH pairs, where the Higgs boson decays to “invisible” final states. Limits have been set assuming that the coupling of the 125 GeV scalar with the W and Z bosons does not exceed the SM predictions, and are shown in the last row of the figure.

In a different model, only two parameters are left free in the fit: κ_V ($\kappa_V = \kappa_W = \kappa_Z$) and κ_F ($\kappa_F = \kappa_t = \kappa_b = \kappa_\tau = \kappa_g$), that measure the Higgs boson couplings to elementary bosons and fermions, respectively, in units of the Standard Model prediction. The result of this fit is shown in figure 3 (right), for the individual channels and for their overall combination.

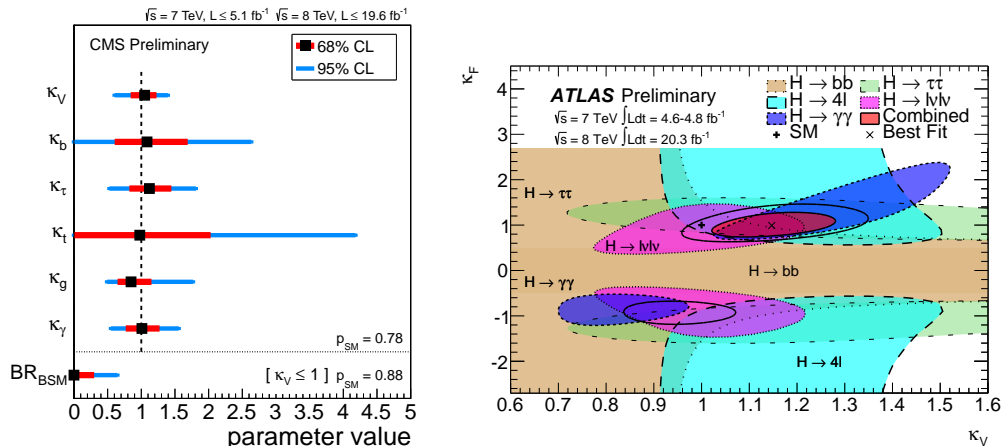


Figure 3: Left: Summary of the fits for deviations in the coupling for the benchmark models in reference [30]. For each model, the best fit values of the most interesting parameters are shown, with the corresponding 68% and 95% CL intervals. The list of parameters for each model and the numerical values of the intervals are provided in reference [26]. Right: Results of fits for the 2-parameter benchmark model defined in Section 5.2.1 of reference [29] that probe different coupling strength scale factors for fermions and vector bosons, κ_V and κ_F , assuming only SM contributions to the total width, overlaying the 68% C.L. contours derived from the individual channels and their combination.

Studies of quantum numbers of the 125 GeV Higgs boson have been presented and discussed. In particular, the spin-parity hypothesis $J^P = 0^+$ has been tested against alternative hypotheses such as $J^P = 0^-, 1^+, 1^-$, as well as against some graviton-inspired $J^P = 2^+$ and 2^- scenarios [31]. Results have been shown by ATLAS, CMS and D0. All tested alternative spin hypotheses appear disfavored compared to the hypothesis $J^P = 0^+$ at more than 97.8% confidence level.

A direct measurement of the Higgs boson natural width Γ_H , predicted by the Standard Model to be $\Gamma_H = 4.15 \text{ MeV}$ for $m_H = 125.6 \text{ GeV}$, is not possible at LHC, because of the experimental mass resolution. However, it has been shown [33][32] that it is possible to constraint the size of Γ_H measuring the ZZ production rate for invariant mass values away from the resonance. Using 4-lepton final states and 2-lepton + missing transverse energy final states, CMS presented an upper limit $\Gamma_H \leq 22 \text{ MeV}$ at 95% confidence level [34]; a similar result has been presented by ATLAS [35].

Beyond Standard Model physics in the Higgs sector has been largely probed following two orthogonal paths: performing direct searches for partners of recently discovered scalar, predicted by a large number of models that extend the Standard Model, and testing these models using the available data on Higgs boson rates. No evidence of new objects associated to the newly discovered particle has been found in searches performed at LHC and Tevatron [36][37][38][39][40][41].

6 Searches beyond Standard Model

Supersymmetry (SUSY) provides an elegant solution to cancel the quadratic mass divergences that would accompany a Standard Model Higgs boson by introducing supersymmetric partners of all SM particles, such as a scalar partner of the top quark, the top squark \tilde{t} . The viability of the of SUSY as a scenario to stabilize the Higgs potential and to be consistent with electroweak naturalness is tested by the search for \tilde{t} below the TeV scale. An example of a nice summary of direct top squark at LHC with the ATLAS detector is available in figure 4 (right). Top squarks with masses between 200 GeV and 700 GeV decaying to an on-shell t-quark and a neutralino are excluded at 95% confidence level for a light neutralino. Similar results have been shown by CMS, and this is now challenging the naturalness of this theory, that represents one of

its strongest points.

Other extensive searches for new physics objects predicted by SUSY implementations have been presented and discussed. Particularly important are also the new results dedicated to the searches for electroweak production of charginos, neutralinos and sleptons. A variety of signatures with leptons, W, Z and Higgs bosons have been investigated by CMS [43], while ATLAS has looked to final states with two leptons and large missing transverse energy [44]. No significant excess beyond Standard Model expectations has been observed, and limits have been set on the masses of charginos and neutralinos in simplified models.

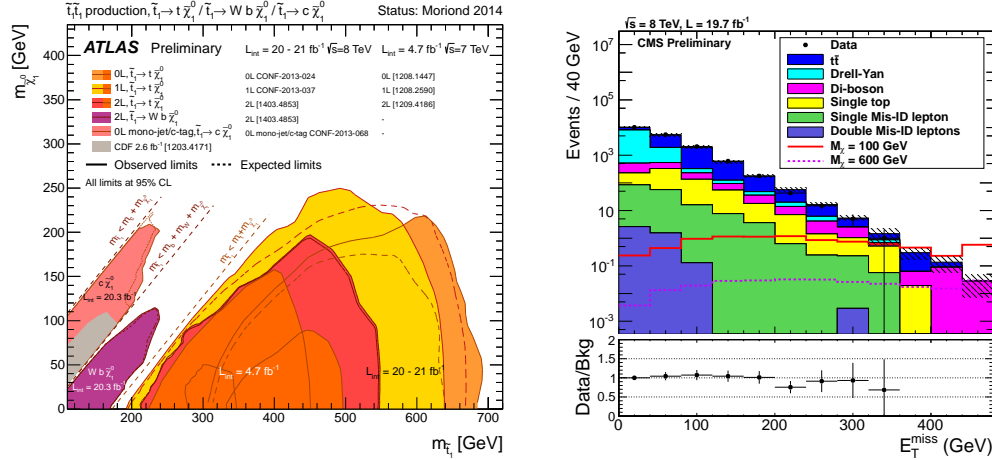


Figure 4: Left: summary of the dedicated ATLAS searches for top squark pair production based on 20-21 fb⁻¹ of pp collision data taken at $\sqrt{s} = 8$ TeV, and 4.7 fb⁻¹ at $\sqrt{s} = 7$ TeV. For more details, see [42]. Right: Distributions of the E_T^{miss} after applying selection cuts. In this figure, two simulated dark matter signals with mass $M_X = 100$ GeV and 500 GeV and the interaction scale $M_* = 100$ GeV are included for comparison. The shaded region represents the total uncertainty of the background prediction. The error on the data-over-background ratio takes into account both the statistical uncertainty of data and the total uncertainty of background [45]. The last bin includes the overflow.

Many searches on non-SUSY beyond-Standard-Model signatures have been presented and discussed. These include investigation of final states of heavy bosons W' and Z' decaying to lepton and heavy quark final states, as well as SM boson pairs. Other phenomena such as events produced by new contact interactions have been probed. No excess of events with respect to the expected yield has been found, and exclusion limits have been set on the mass of new particles predicted by several BSM models, or on the energy scale at which new forces could appear.

Dark matter searches are one of the central subjects of BSM studies at LHC. Many theories predicts dark matter particles light enough to be produced by this collider. If produced, these objects would escape the detector producing a large missing transverse energy. In some particular implementation, dark matter particle pairs are produced in association with top-antitop pairs, whose leptonic decays can be used to tag the events. Figure 4 (right) shows the distribution of E_T^{miss} after selections cuts for data and predictions, showing no evidence for production of new physics in this type of investigations [45].

7 Heavy Ion physics

Many new - and often unexpected - results have been presented at this Conference. Quite a few of them are related to p-Pb collision studies, made with data collected a couple of years ago at $\sqrt{s_{NN}} = 2.76$ TeV. Among these, the analysis of the *ridge* performed using pp, PbPb and pPb data, and comparing the respective findings, has shown surprising results. As long-range correlations are seen in both PbPb and pp collisions,

it was natural to expect a possible effect also in pPb collisions. However, within a week of data-taking it appeared already clear that the correlations in pPb are surprisingly much stronger than in pp collisions [46]. A large set of measurements strongly suggest that the ridge(s) results seem to indicate that the same collective physics that we think we understand in PbPb is present also in pp and pP on soft scales.

Another major topic discussed was the measurement of the single jet suppression, to to the propagation of partons in the hot dense medium of quark-gluon plasma (QGP) produced in heavy ion collisions. This is done measuring the jet yield in a given p_T and centrality bin, and rescaling taking into account the number of nucleon-nucleon collisions expected for that bin. The data analysed are from a sample of inclusive jets produced in PbPb collisions at $\sqrt{s_{NN}} = 2.76$ TeV. The ratio R_{CP} of yields measured at different centralities to the one observed in the centrality bin 60%-80% is determined and plotted as a function of the reconstructed jet p_T . A factor ~ 2 suppression in jet rate is observed [48]; see also figure 5 (left).

Heavy quarks are an important probe of the QGP since they are expected to be produced only during the initial stage of the collision in hard partonic interactions, thus experiencing the entire evolution of the system. It was predicted that in a hot and dense deconfined medium like the QGP, bound states of charm and anti-charm quarks, i.e. charmonia, are suppressed due to the screening effects induced by the high density of color charges. The relative production probabilities of charmonium states with different binding energies may provide important information on the properties of this medium and, in particular, on its temperature. Among the charmonium states, the strongly bound $J\psi$ is of particular interest [47]. The behaviour of the nuclear modification factor, R_{AA} , as a function of the centrality $\langle N_{part} \rangle$ shown in figure 5 (right) indicates that for increasing values of this variable, a constant value of R_{AA} is observed, suggesting some type of regeneration processes. The charmonium loses the status of “thermometer” of the QGP medium, and may play an important role in the the understanding of the phase boundary.

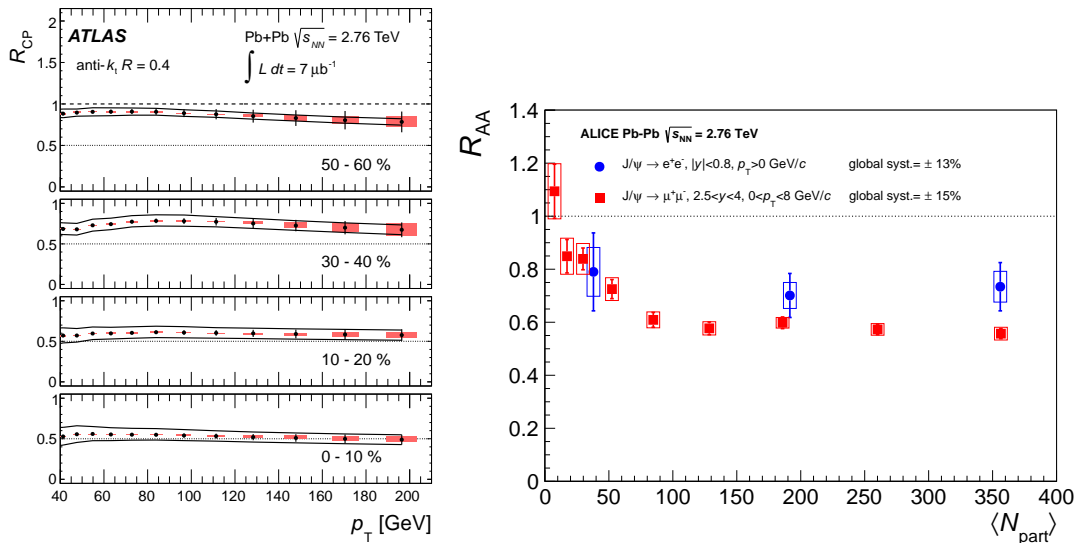


Figure 5: Left: Unfolded R_{CP} values as a function of jet p_T for $R = 0.4$ anti-kt jets in four bins of collision centrality. The error bars indicate statistical errors from the unfolding, the shaded boxes indicate unfolding regularization systematic errors that are partially correlated between points. The solid lines indicate systematic errors that are fully correlated between all points. The horizontal width of the systematic error band is chosen for presentation purposes only. Dotted lines indicate $R_{CP} = 0.5$, and the dashed lines on the top panels indicate $R_{CP} = 1$ [48]. Right: Centrality dependence of the nuclear modification factor, R_{AA} , of inclusive $J\psi$ production in Pb-Pb collisions at $\sqrt{s_{NN}} = 2.76$ TeV, measured at mid-rapidity and at forward rapidity [48].

8 Future Prospects

The LHC machine is in shutdown since March 2013, mainly for magnet interconnect repairs, to allow nominal current in the dipole and lattice quadrupole circuits of the LHC [49]. This should bring the collision energy to a value close to $\sqrt{s} = 14$ TeV. The instantaneous luminosity will increase up to the nominal value $\mathcal{L} = 10^{34}$ $\text{cm}^{-2}\text{s}^{-1}$, and will be doubled with another machine upgrade planned for 2018. The LHC will accumulate data corresponding to an integrated luminosity of about 300 fb^{-1} by 2022, or so.

To extend its discovery potential, the LHC will need a major upgrade to increase its luminosity by a factor of 5 (or more) beyond its design value. As a highly complex and optimized machine, such an upgrade of the LHC must be carefully studied and requires about 10 years to implement.

The novel machine configuration, the High-Luminosity LHC (HL-LHC), will rely on a number of key innovative technologies, representing exceptional technological challenges, such as a few cutting-edge 13 Tesla superconducting magnets, very compact and ultra-precise superconducting cavities for beam rotation, and 300-metre-long high-power superconducting links with zero energy dissipation [50][51][52].

With this final upgrade, the LHC machine should deliver an integrated luminosity of about 3000 fb^{-1} per experiment (ATLAS and CMS) by ~ 2030 , see figure 6 (left).

With this ultimate data set, the HL-LHC will be the unique worldwide facility to look for rare processes and it will give an unprecedented sensitivity for a large range of the newly discovered Higgs boson property measurements, as well as for searches for new particles and precision studies for a wide set of fundamental physics processes [53].

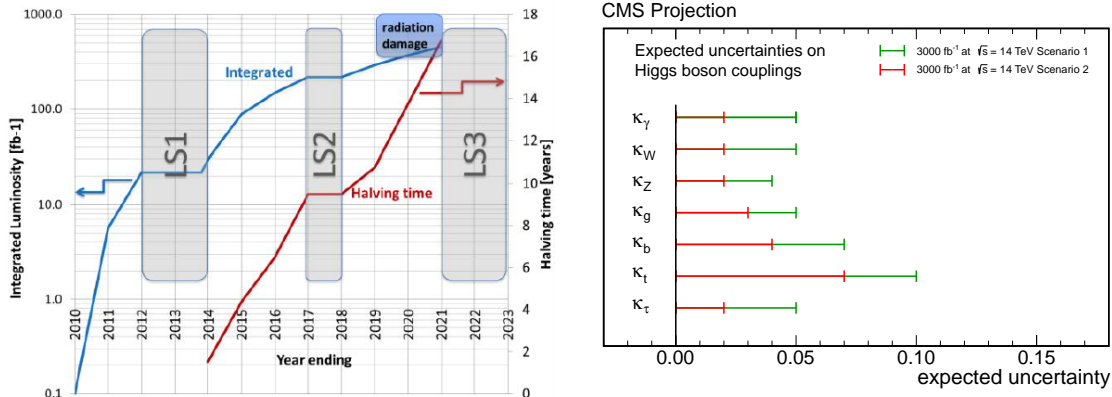


Figure 6: Left: Integrated luminosity and running time to reduce by a factor two the statistical error based on flat luminosity (halving time). Superimposed the three long shutdowns and the area where it is expected that radiation damage will call for changing of the low- β quadrupoles (also called inner triplet). Right: Estimated precision on the measurements of κ_γ , κ_W , κ_Z , κ_g , κ_b and κ_τ . The projections assume $\sqrt{s} = 14$ TeV, a dataset corresponding to 3000 fb^{-1} and that no particles other than those from SM contribute to the Higgs boson natural width or to the loops. Furthermore, Scenario 1 assumes current experimental and theoretical uncertainties, while Scenario 2 assumes that these uncertainties scale with $1/\sqrt{L}$ (where L is the integrated luminosity) and $1/2$, respectively.

Figure 6 (right) shows the expected accuracy on the 125 GeV Higgs boson couplings computed by CMS [54]; ATLAS has shown very similar results [55].

9 Conclusions

The first run of LHC has shown outstanding performance of the machine and of the ALICE, ATLAS, CMS and LHCb detectors. High-quality results have been produced in high- p_T , heavy flavour and heavy ion

physics. A new boson, compatible within experimental and theoretical uncertainties with the Standard Model Higgs boson, has been observed at a mass of about 125 GeV.

The collaboration of experimentalist and theorist communities has played an important role in understanding current data, and it will be essential also in future.

The LHC has shown that hadron colliders can do not only new physics searches, but also precision physics, as already demonstrated by the experiments at Tevatron.

As of today, we analysed less than 10% of the dataset expected from LHC, and at a centre-of-mass energy about half of the energy of future LHC runs, starting from 2015. Furthermore, ultimate LHC precision studies to probe for new physics effects at the TeV scale can be performed with the luminosity upgrade of the machine and of the detectors.

With the new start of LHC after the long shutdown of 2012-2014, we are entering a new era in HEP, with the LHC acting as a “portal” to a possible new world.

References

- [1] S. Chatrchyan *et al.* [CMS Collaboration], Phys. Rev. D **90**, 032008 (2014) [arXiv:1404.4619 [hep-ex]].
- [2] G. Aad *et al.* [ATLAS Collaboration], arXiv:1405.6241 [hep-ex].
- [3] M. Czakon, M. L. Mangano, A. Mitov and J. Rojo, JHEP **1307**, 167 (2013) [arXiv:1303.7215 [hep-ph]].
- [4] ATLAS Collaboration, ATLAS-CONF-2014-007 (2014).
- [5] V. Khachatryan *et al.* [CMS collaboration], Phys. Rev. Lett. **112**, 231802 (2014) [arXiv:1403.7366 [hep-ex]].
- [6] S. Chatrchyan, *et al.* [CMS collaboration], JHEP **1406**, 090 (2014) [arXiv:1401.2942 [hep-ex]].
- [7] ATLAS Collaboration, ATLAS-CONF-2013-010 (2013).
- [8] ATLAS Collaboration, ATLAS-CONF-2011-118 (2011).
- [9] CMS Collaboration, CMS-PAS-TOP-13-009 (2013).
- [10] T.A. Aaltonen *et al.* [CDF Collaboration, D0 Collaboration], Phys. Rev. Lett. **112**, 231803 (2014) [arXiv:1402.5126 [hep-ex]].
- [11] ATLAS Collaboration, CDF Collaboration, CMS Collaboration, D0 Collaboration, arXiv:1403.4427 [hep-ph].
- [12] S. Moch, “Top theory,” these proceedings.
- [13] S. Moch, S. Weinzierl, S. Alekhin, J. Blumlein, L. de la Cruz, *et al.*, arXiv:1405.4781 [hep-ph].
- [14] N. Cabibbo, Phys. Rev. Lett. **10**, 531 (1963).
- [15] M. Kobayashi, T. Maskawa, Prog. Theor. Phys. **49**, 652 (1973).
- [16] R. Aaij *et al.* [LHCb collaboration], Phys. Rev. Lett. **112**, 011801 (2014) [arXiv:1310.4740 [hep-ex]].
- [17] R. Aaij *et al.* [LHCb collaboration], Phys. Rev. Lett. **111**, 101801 (2013) [arXiv:1306.1246 [hep-ex]].
- [18] M. Bobrowski, A. Lenz, J. Riedl, J. Rohrwild, JHEP **1003**, 009 (2010) [1002.4794 [hep-ph]].
- [19] R. Aaij *et al.* [LHCb collaboration], JHEP **1407**, 041 (2014) [arXiv:1405.2797 [hep-ex]].
- [20] G. Aad *et al.* [ATLAS Collaboration], Phys. Lett. B **716**, 1 (2012) [arXiv:1207.7214 [hep-ex]].
- [21] S. Chatrchyan *et al.* [CMS Collaboration], Phys. Lett. B **716**, 30 (2012) [arXiv:1207.7235 [hep-ex]].

- [22] G. Aad *et al.* [ATLAS collaboration], submitted to Phys. Rev. D [arXiv:1406.3827 [hep-ex]].
- [23] G. Aad *et al.* [ATLAS collaboration], submitted to EPJC [arXiv:1407.5063 [hep-ex]].
- [24] CMS Collaboration, CMS-PAS-HIG-13-001 (2013).
- [25] S. Chatrchyan *et al.* [CMS collaboration], Phys. Rev. **D89**, 092007 (2014) [arXiv:1312.5353 [hep-ex]].
- [26] CMS Collaboration, CMS-PAS-HIG-13-005 (2013).
- [27] CMS Collaboration, CMS-PAS-HIG-14-009 (2014).
- [28] S. Chatrchyan *et al.* [CMS collaboration], Nature Phys. **10**, (2014) [arXiv:1401.6527 [hep-ex]].
- [29] ATLAS Collaboration, ATLAS-CONF-2014-009 (2014).
- [30] S. Heinemeyer *et al.* [LHC Higgs Cross Section Working Group Collaboration], arXiv:1307.1347 [hep-ph].
- [31] S. Bolognesi, Y. Gao, A. V. Gritsan, K. Melnikov, M. Schulze, N. V. Tran and A. Whitbeck, Phys. Rev. D **86**, 095031 (2012) [arXiv:1208.4018 [hep-ph]].
- [32] F. Caola and K. Melnikov, Phys. Rev. D **88**, 054024 (2013) [arXiv:1307.4935 [hep-ph]].
- [33] N. Kauer and G. Passarino, JHEP **1208**, 116 (2012) [arXiv:1206.4803 [hep-ph]].
- [34] V. Khachatryan *et al.* [CMS Collaboration], Phys. Lett. B **736**, 64 (2014) [arXiv:1405.3455 [hep-ex]].
- [35] ATLAS Collaboration, ATLAS-CONF-2014-042 (2014).
- [36] CMS Collaboration, CMS-PAS-HIG-13-021 (2013).
- [37] G. Aad *et al.* [ATLAS Collaboration], JHEP **1302**, 095 (2013) [arXiv:1211.6956 [hep-ex]].
- [38] R. Aaij *et al.* [LHCb Collaboration], JHEP **1305**, 132 (2013) [arXiv:1304.2591 [hep-ex]].
- [39] V. M. Abazov *et al.* [D0 Collaboration], Phys. Lett. B **710**, 569 (2012) [arXiv:1112.5431 [hep-ex]].
- [40] T. Aaltonen *et al.* [CDF and D0 Collaborations], Phys. Rev. D **86**, 091101 (2012) [arXiv:1207.2757 [hep-ex]].
- [41] S. Chatrchyan *et al.* [CMS Collaboration], Phys. Lett. B **722**, 207 (2013) [arXiv:1302.2892 [hep-ex]].
- [42] https://atlas.web.cern.ch/Atlas/GROUPS/PHYSICS/CombinedSummaryPlots/SUSY/ATLAS_SUSY_Stop_tLSP/history.html.
- [43] V. Khachatryan *et al.* [CMS Collaboration], arXiv:1405.7570 [hep-ex].
- [44] G. Aad *et al.* [ATLAS Collaboration], JHEP **1405**, 071 (2014) [arXiv:1403.5294 [hep-ex]].
- [45] CMS Collaboration, CMS-PAS-B2G-13-004 (2013).
- [46] W. Li, "Flow and soft phenomena in heavy-ion collisions," these proceedings.
- [47] A. Betty Bezverkhny *et al.* [ALICE Collaboration], Phys. Lett. B **743**, 314 (2012) [arXiv:1311.0214 [nucl-ex]].
- [48] G. Aad *et al.* [ATLAS Collaboration], Phys. Lett. B **719**, 220 (2013) [arXiv:1208.1967 [hep-ex]].
- [49] F. Bordry, "LHC status and prospects," these proceedings.
- [50] L. Rossi and O Brning, CERN-ATS-2012-236.
- [51] <http://hilumilhc.web.cern.ch/HiLumiLHC/index.html>

- [52] L. Rossi, Proceedings of IPAC2011 conference, San Sebastian, Spain, <https://accelconf.web.cern.ch/accelconf/IPAC2011/papers/tuya02.pdf>.
- [53] D. Abbaneo *et al.* [Report submitted to ECFA Prepared from inputs provided by the ALICE, ATLAS, CMS and LHCb Collaborations 21st November 2013], Physics and Technology Challenges,” ECFA/13/284.
- [54] [CMS Collaboration], arXiv:1307.7135.
- [55] ATLAS Collaboration, ATLAS-PHYS-PUB-2013-004 (2013).